

# Development of an imaging system for spatially real-time measurement of drying parameters in industrial drying units

Waseem Amjad<sup>1\*</sup>, Anjum Munir<sup>1</sup>, Barbara Sturm<sup>2</sup>

(1. Department of Energy Systems Engineering, University of Agriculture Faisalabad, Pakistan;

2. Department of Agricultural and Biosystems Engineering, University of Kassel, Germany)

**Abstract:** Lack of accurate information for the drying kinetics is the main barrier to optimize drying processes effectively. Online monitoring of drying data is not common due to practical issues involved in set-up application. In this study an imaging system was developed for large drying units to investigate the quality changes (color kinetics and shrinkage) combine with weight loss of food product spatially and non-destructively during convective drying. The imaging setup was used in a diagonal-airflow batch dryer and shifted along the dryer length to take data (food images and weight loss) at different positions using potato slices (5 mm thick, 60°C) as drying material. First order model fitted well to value of  $\Delta L^*$  and  $\Delta b^*$  while  $\Delta a^*$  and  $\Delta E$  fitted in the zero order model. The experimental and models predicted color kinetics revealed good correlation coefficients ( $R^2 = 0.88-0.99$ ,  $P < 0.0001$ ). The shrinkage of the samples exhibited two periods; a faster with moisture ration (MR) up to 0.3 and afterwards it became slow employing polynomial cubic regression ( $R^2 = 0.97-0.99$ ,  $P < 0.0001$ ). The imaging system effectively measured the change in quality parameters spatially along the dryer. The current study would help to develop and implement low cost setup for online measurements used for the assessment of drying processes in large drying units.

**Keywords:** image processing, real time data, drying

**Citation:** Amjad, W., A. Munir, and B. Sturm. 2020. Development of an imaging system for spatially real-time measurement of drying parameters in industrial drying units. *Agricultural Engineering International: CIGR Journal*, 22 (4):238-249.

## \* 1 Introduction

The rate of moisture removal is an important factor regarding the final achievable quality of dried materials. It depends on several factors, including the drying medium, initial moisture content of the raw material, type of the product, relative humidity, velocity and importantly the drying temperature. In the food drying, food quality affected by drying temperature has been reported by many investigators (Ramos et al., 2004; Farias et al., 2008; Orikasa et al., 2008; Diamante et al., 2010; Elamin, 2014) showing that drying is a complex

process to be optimized.

In order to define the required/optimum drying conditions for minimum change in product quality, different measuring techniques are applied in food drying processes. Usually, trained visual inspectors evaluate the dehydration level in food quality control which is a tedious, time consuming, costly and unreliable approach (Abdullah et al., 2004). Another approach is sampling and instrumentation that is more precise, but an invasive procedure (Jayas et al., 2000), affect the quality attributes by interrupting the process. A recently evolved non-destructive technique has been the use of computer vision systems (CVSs) for real-time measurement of fruits and vegetables quality parameters, such as color (Yam and Papadakis, 2004; Pedreschi et al., 2006) and shrinkage (Fernandez et al., 2005; Martynenko, 2006) but usually are applied at laboratory scale. During the drying process,

---

**Received date:** 2019-09-03 **Accepted date:** 2019-12-29

\* **Corresponding author:** Waseem Amjad, Ph.D., Assistant Professor of Department of Energy Systems Engineering, University of Agriculture Faisalabad, 38000 Pakistan., Email: waseem\_amjad@uaf.edu.pk. Tel: (+92) 41-9200161-3016.

biological materials show varying characteristics even with the same operating conditions due to their heterogenic nature (Nazghelichi et al., 2011). Often the product temperature is unknown or assumed to be constant or if it is measured, it is not included in the process control system (Mujumdar and Law, 2009; Sturm, 2010). However, several studies on fruit and vegetable (Sturm et al., 2012; Nunez et al., 2016) show that product temperature changes throughout the drying process for product with high initial moisture contents like potato. Therefore, for product quality and process assessment, drying parametric changes should be monitored accurately. The main hindrance for the development of a control strategy for a convective drying process is the lack of accurate information for the drying kinetics of the respective product. This is due to the use of conventional and inappropriate methods for gaining such information which results in the inability to ensure the desired progress of a process. It is evident from a survey of recent research papers published in *Food and Bioprocess Technology*: that out of the 29 articles, the majority (58.62%) used a Minolta colorimeter, 24.14% used a Hunter-Lab instrument, and 17.24% used other types of instruments (mixed) for the measurement of color attributes in the drying process (Pathare et al., 2012). Accurate information of a drying process is required for a better automatic control of drying process important to reduce drying time and energy (Groß et al., 2011). Although the application of such tools has been reported by some researchers (Pathare et al., 2012) but for laboratory scale drying units. Therefore, research on the development of affordable and applicable sensors for spatial real-time measurements of drying data, such as color change in large processing units is the need. Secondly, none of the study has been reported for the combine estimation of quality changes and weight loss non-invasively in large batch food dryers.

Potato is one of the most consumed vegetables in the world. Dried potatoes can be used to make various products and normally convective drying is used to dry that product. However, it causes undesirable thermal degradation of the product quality for which temperature is the main influencing factor (Chen and Mujumdar,

2008). Measurement of color degradation (Chua et al., 2002) and shrinkage (Khraisheh et al., 1997; Mclaughlin and Magee, 1998) during convective drying of potato has been reported by many researchers using destructive approaches. Application of non-invasive technologies for the potato processing mainly focused to sorting and grading based on color, size and shape (Narendra and Hareesh, 2010; Mahendran et al., 2012; Avila and Silva, 1999; El-Masry et al., 2012; Hassankhani and Navid, 2012). However, less data is available on color degradation and shrinkage of potato slices during air drying using non-invasive method and most of the reported works deal with shrinkage measurement. Wang and Brennan (1995) used light microscopy to study the structural changes in potato during drying. They developed a model to represent the relationship between the density and moisture content. Mulet et al. (2000) measured shrinkage of potato cubes, parallelepipeds and cylinders using an image setup and a calliper and showed a good agreement between the two methods. Alireza et al. (2009) reported a computer vision based methodology to study the effect of drying conditions on product shrinkage. The study revealed that rate of shrinkage of product (potato slices) reduced with moisture content in the directly proportional relationship. Mendiola et al. (2007) measured non-isotropic shrinkage in potato slabs at its top and side using two digital cameras. The measured area (surface) of potato cells was plotted against moisture content using an empirical equation. Shekofteh et al. (2012) studied the effect of moisture on shrinkage of cylindrical potato pieces (10 mm thick, 35 mm diameter) and found non-uniform shrinkage at temperatures of 60°C and 70°C whiles uniform shrinkage (very similar to the circle-shape mode) at 80°C. Based on a detailed literature review, no work has been reported for on-line monitoring of potato slices color kinetics during convective drying. A thorough understanding of the various changes in color of potato slices during convective drying can provide an appropriate approach to optimize the drying process and hence minimize the degradation of quality attributes. Therefore, the potato was selected as drying material to assess the functionality of an imaging box system.

The objectives of the current study were to develop an imaging system capable of precise assessment of the drying kinetics and food quality changes (color and shrinkage) spatially applied to a diagonal-airflow batch type dryer. Real-time monitoring of color kinetic and shrinkage were investigated to develop their relationships with dimension less moisture content of the product. The study will provide a low cost optical online measuring technique for large convective food dryers. The outcomes will help to optimize the drying conditions in a better way for the used dryer to get productive with minimal change in the final quality.

## 2 Materials and methods

### 2.1 Dryer used

Figure 1 shows a diagonal-batch dryer that was used for the current study. It consists of three major components are called connector, lower half, and upper half, the drying chamber. The heating chamber is made beneath the drying chamber to reduce space requirements. A connector is used to connect the lower half to the upper half of the dryer. In the drying chamber, twenty-five food buckets (each of size, 0.6 m×0.4 m×0.29 m) each with four perforated trays were arranged diagonally on a rolling track (for easy loading and unloading of food buckets). These diagonally arranged buckets gave a shape of the diagonal airflow channel at an angle of  $1.42^\circ$  with the wall of the drying chamber in the longitudinal direction as shown in Figure 1.

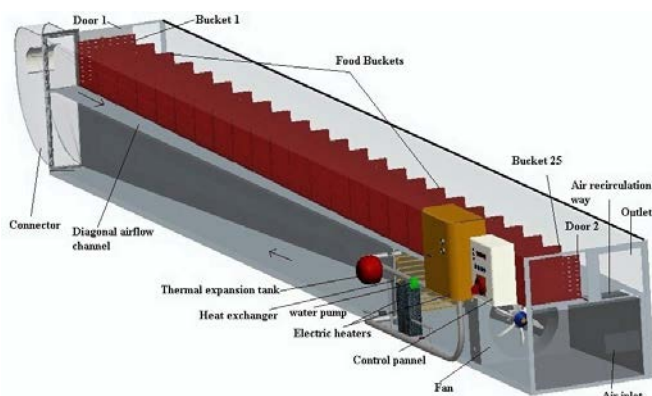


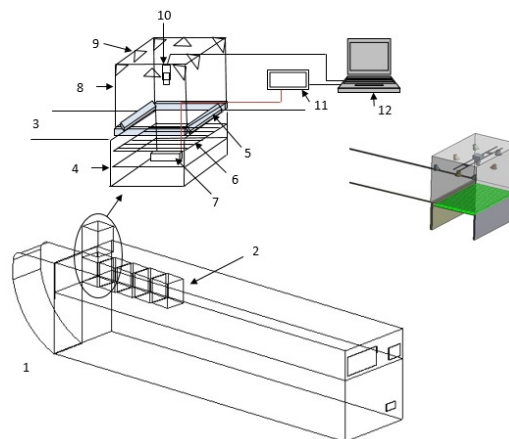
Figure 1 Diagonal-batch type food dryer (Amjad and Munir, 2015)

This channel acts as inlet for all the buckets, so all the food materials get uniform exposure to the drying air. A rectangular passage (0.30 m×0.15 m) was installed just before the outlet door (0.30 m×0.15 m) for air

recirculation. A control panel was used to set the temperature and time (three different temperatures can be set for three different intervals of drying time for a drying process). The detailed numerical and experimental based functional description of the dryer has been reported by Amjad and Munir (2015).

### 2.2 Data acquisition system

The frame of the image acquisition system was made of a wooden box having an area equal to the size of a food bucket (0.6 m×0.4 m), Color Autofocus Camera (DFK 72AUC02-F) a USB CMOS MT9P031 sensor (Lens mount M12x0.5) and a computer (Lenovo T500, 2.40 GHz) as shown in Figure 2.



(1) batch dryer (2) diagonally arranged food buckets (3) roof (4) bucket (5) acrylic sheet (6) food tray (7) load cell (8) imaging box (9) lights (10) camera (11) data logger (12) computer.

Figure 2 Schematic layout of real time data monitoring system

For light, eight LED bulbs (each of equal to 60 watts) were used for uniform distribution of light over the food tray in order to get sharp contrast through avoiding glitter. To capture diffuse reflection, an angle of  $45^\circ$  was kept between the axis of the camera lens and light source (Fernandez et al., 2005). The height of the bars, holding the camera within the imaging box, was defined as per required gap (42 cm) between the lens and food sample for best quality image (high contrast and pixel resolution). The inner walls of the box painted black to avoid reflection of the room. The top of the drying chamber in place of the first food bucket was cut into to position imaging-box over it. A transparent acrylic sheet was put at the bottom of the box to prevent the air to flow into the box and to allow transmission of the light to the target position (food tray) as shown in Figure 2.

### 2.3 Drying experiments

Potatoes (variety: Anuschka) were used to study their color kinetics and shrinkage in real time measurement and assess the functionality of the developed imaging system. Before slicing, product was washed, peeled and then sliced using an electric slices (Bosch MAS62) into 5 mm thickness. In order to reduce enzymatic reactions, the slices were blanched in boiling water for a period of three minutes. After cleaning surface water with a clean cloth, blanched slices (half a kilogram) were put on food tray that was connected to load cell. The drying temperature was set at 60°C and product was dried to a 12% final moisture content. imaging system continuously captured the images (2048×1536 pixels) of potato slices with a time interval of five minutes as shown in Figure 3.



Figure 3 Imaging-box system made for data acquisition

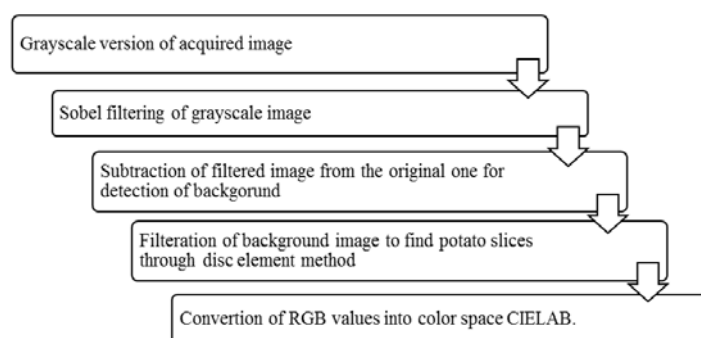
IC Capture-2.4 software was used for digital data output and saved in TIFF format via the USB interface. Similarly, change in weight loss of potato slices was also recorded continuously (five minutes time intervals) by load cell via data logger and the results were saved in CSV (Comma separated values) format. The dryer’s length was divided into five sections of 2 m each in length and comprising five buckets. So the data presented

in a section is the average value of data measured from the five buckets.

### 2.4 Calibration of the imaging system (color camera)

Color calibration of the RGB camera (The Imaging Source, Germany) was achieved through the polynomial color correction (Finlayson et al., 2015b). An X-Rite Color Checker Classic 24 patch chart (X-Rite Inc., Michigan, USA) was imaged using a set exposure. Polynomial color correction rather than root polynomial color correction (Finlayson et al., 2015a) was utilized due to the use of a single exposure for imaging during the drying process. The reflectance and colorimetric data of each patch was then measured using a calibrated spectrometer (Q mini, RGB Photonics GmbH, Kelheim, Germany). The measured colorimetric XYZ values were then regressed alongside the measured average patch RGB values after subtraction of the average black patch RGB values. This produced a polynomial function which allowed the calculation of XYZ coordinates from measured RGB values. These calculated XYZ values were then converted into CIELAB coordinates using illuminant D65 as the reference white point, with a luminance value equal to the luminance of the white patch under the test illumination.

### 2.5 Image analysis for of color and shrinkage features extraction



RGB color measurement is affected by the camera sensitivity and light source (Leon et al., 2006). Acquiring an effective image depends on computer techniques and model used to obtain information from these acquired images and it involved many steps line pre-processing, separation of object from background, conversion of RGB images into color space. For this, a program was written in MATLAB code. The followed steps in this

process are described below and also graphically presented in Figure 4.

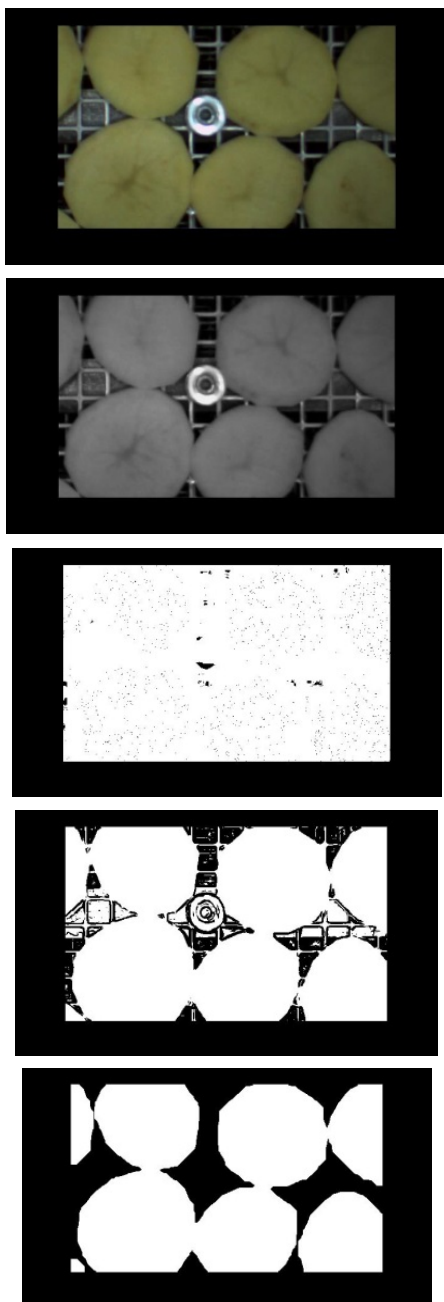


Figure 4 Steps involved in the image analysis process for color data

The light was more uniform in the middle of the tray so this part was used for color detection. The color space, i.e. CIE  $L^*$ ,  $a^*$ ,  $b^*$  is broadly used in food related research because it gives consistent output in the form of color (Yam and Papadakis, 2004). The average values of the extracted colors were expressed in the *CIELAB* color space system as  $L^*$  (lightness/darkness),  $a^*$  (redness/greenness) and  $b^*$  (yellowness/blueness). In order to normalize parameters for decreasing difference among different raw samples, ratios of  $L^*$ ,  $a^*$ , and  $b^*$  to the corresponding initial values were calculated (Sahin,

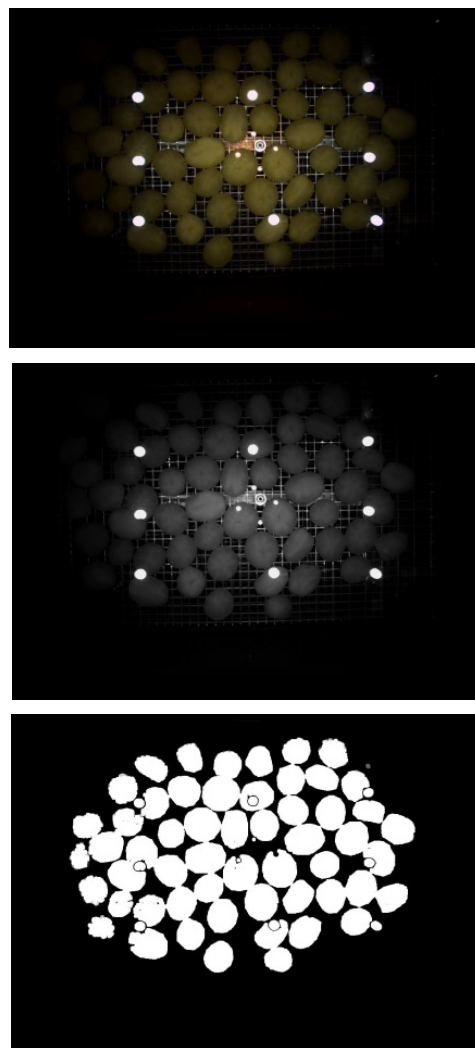
2006). Total color difference ( $\Delta E$ ) is being widely reported for the determination of color change in drying processes. Following equation was used (Sturm, 2014).

$$\Delta E = [(L_0^* - L^*)^2 + (a_0^* - a^*)^2 + (b_0^* - b^*)^2]^{0.5} \quad (1)$$

Where  $L^*$ ,  $a^*$  and  $b^*$  with subscript "o" stand for respective color values of fresh samples while  $L^*$ ,  $a^*$  and  $b^*$  represent the color values measured at time  $t$  during the drying process.

For shrinkage calculation the followed steps are presented in Figure 5. The number of potato pixels in the image were then counted. For each bucket the number of potato pixels was then normalized to 1 with the number of potato pixels recorded at the start of the drying process.

Shrinkage measurements were made from the entire food tray. The systematic error was inevitable because of the reflection of lights across the tray. The lightning arrangement should be close to the acrylic sheet for better light distribution uniformity over the tray.



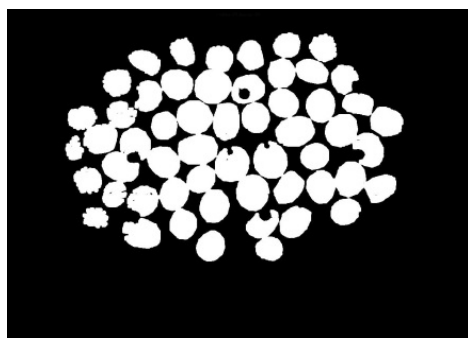


Figure 5 Steps involved in the image analysis process for potato slices shrinkage calculation

### 2.6 Color kinetic

Food product undergoes continuous changes in a drying process so kinetic information of desired parameters becomes important to estimate. For the assessment and modelling of color changes, application of zero and first order kinetic models are best to use (Sturm et al., 2014; Mujumdar, 2000). For this, so, the following equations were used.

$$C = C_o \pm k_o t \tag{2}$$

$$C = C_o \exp(\pm k_1 t) \tag{3}$$

Where  $C$  is the measured value of color variables ( $L^*, a^*, b^*$ ) at time  $t$ ,  $C_o$  is the initial value of color variables at the start,  $t$  is the drying time,  $k_o$  is the zero-order kinetic constant and  $k_1$  is the first-order kinetic constant. The positive and negative signs indicate formation and degradation of the quality parameter respectively.

## 3 Results and discussions

### 3.1 Drying kinetics

Figure 6 shows the drying curves for potato slices based on the weight data measured non-destructively using the load cell.

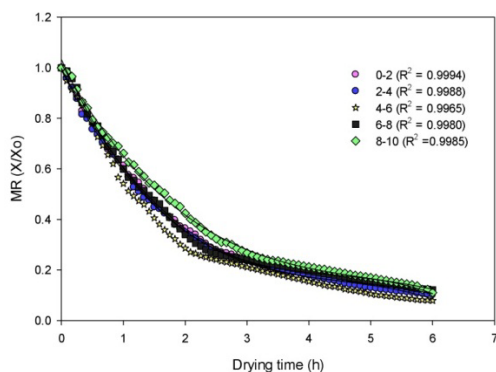


Figure 6 Drying characteristic curves at different sections of drying chamber

The moisture content of the product was plotted as moisture ratio with drying time during the drying process. The rate of moisture removal was high during the first two and half hours of the drying time, followed by a decreased rate of drying for the rest of the drying process. The moisture ratio (MR) data as a function of drying time for all five positions within the drying chamber were fitted well using the polynomial cubic model (based on  $R^2$  values).

### 3.2 Color kinetics

#### 3.2.1 Lightness difference ( $\Delta L^*$ )

Figure 7a shows change in lightness attribute of potato slices with respect to their moisture change during the drying process. It shows that the lightness difference ( $\Delta L^*$ ) increased with drying time as the moisture of the product decreased for all the sections showing that the value of  $L^*$  decreased continuously with respect to the reference value (initial value of  $L^*$ ). The reduced level of brightness in the dried product could be considered as a measurement of browning, which occurred due to an increased lightness difference from 0.05-11.67, 0.58-10.22, 0.34-11.07, 0.35-12.30 and 0.09-11.89 for sections 1-5 respectively. It shows that slice inclined to get slightly darker as the drying proceeded and resulted in an increase of the color difference ( $\Delta E$ ). The rate of increase in the lightness difference was observed smooth until  $X/X_o \geq 0.3$  and after that the product's changes in lightness increased.

The decreasing of lightness can also be linked with non-enzymatic browning and brown pigment formation as blanching of potato slices helped to inactivate most of the enzymes (Krokida et al., 1998). The change in structural changes in potato slices (shrinkage) increased opacity in samples which might also be related to decreased values of lightness (Contreras et al., 2008). Pedreschi et al. (2007) reported that the product temperature significantly affects the luminosity of potato slices in inversely proportional relation.

#### 3.2.2 Redness difference ( $\Delta a^*$ )

During the drying process, the change in redness difference ( $\Delta a^*$ ) with respect to dimensionless, moisture content of the product has been shown in Figure 7b. With the passage of drying process, the greenness of potato

slices (low value of  $a_0^*$ ) reduced and samples tended towards redness (high value of  $a_0^*$ ). Occurring of non-enzymatic browning reactions are the main reason for the change in chromatic parameter ( $a^*$ ) of potato slices from its reference value of  $a_0^*$  during the drying process. It can be observed that  $\Delta a^*$  increased with the drying time (decrease of moisture content) and this trend was similar for all the sections of the drying chamber. The negative sign with redness difference indicate the higher values of  $a^*$  from that of initial values at any time of the drying process. Millard browning reactions, increased with the rise of product temperature, which also caused a rise in redness of dried product (Chua et al., 2002). Similar results trend was reported by other researchers for other varieties of potato slices like Panda, Saturna and Bintje (Segnini et al., 1999). The rate of increase in redness difference was observed smooth until  $X/X_0 \geq 0.3$  and after that the product's changes in redness increased.

### 3.2.3 Yellowness difference ( $\Delta b^*$ )

Figure 7c manifests the color difference for the parameter  $b^*$  with moisture ratio ( $X/X_0$ ) at various positions of the drying compartment. With the decreased of moisture ratio from 1 to 0.3, the yellowness difference ( $\Delta b^*$ ) increased from 0.17 to 0.9 throughout the drying chamber. The maximum value of that change rate was observed at  $X/X_0 < 0.3$ . It could be due to the decreased yellowish parts in potato samples resulted due to Millard reactions and browning formations with final values of  $\Delta b^*$  2.47, 2.47, 2.28, 2.50 and 2.10 for dryer's sections 1-5 respectively.

### 3.2.4 Total color difference ( $\Delta E$ )

Figure 7d shows change in total color change with respect to moisture ration for all sections of the drying chamber. It can be seen that with the increase of drying time, i.e. lowering moisture content, the value of  $\Delta E$  increased resulted due to non-enzymatic browning reactions at potato surfaces. Up to a value of moisture ration 0.3, all color attributes ( $L^*, a^*, b^*$ ) were increased gradually and this increasing trend became higher near the end of the drying process. It showed that potato slices have a tendency to lose their brightness and to get darker with the passage of drying time. It should be noted here

that change in a variety of product used would also affect the rate of color change (Hatamipour et al., 2007).

Overall, among the five sections of the drying chamber, values of total color difference were calculated in the ranged of 13-17.

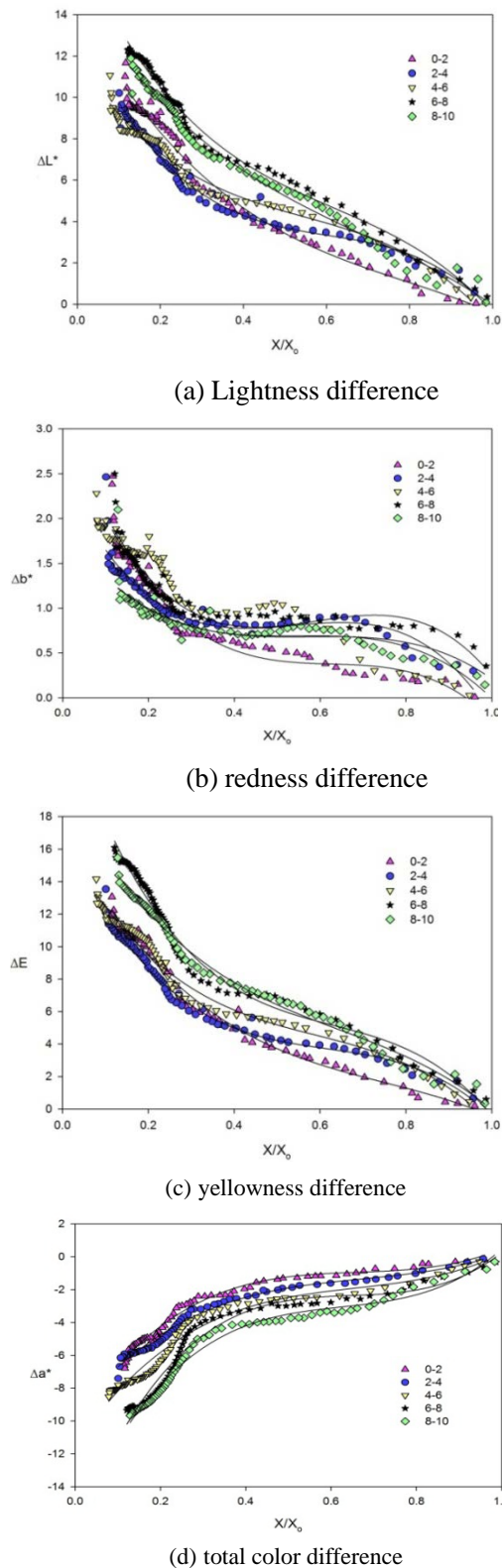


Figure 7 Color differences with respect to moisture content at different sections of drying chamber

**Table 1** Obtained outcomes for the model fitting of investigating parameters

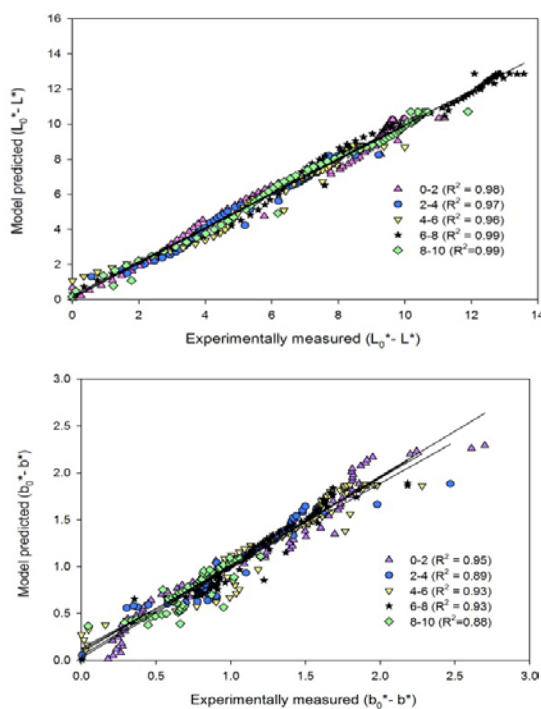
Parameter	Section	$y_0$ (intercept)	a	b	c	$R^2$	SEE
$\Delta L^*$	0-2	14.219	-	37.549	15.779	0.9836	0.427
	2-4	13.547	-	68.613	37.961	0.9864	0.286
	4-6	11.831	-	45.848	27.965	0.9738	0.367
	6-8	17.186	-	56.366	30.406	0.9906	0.322
	8-10	15.094	-	33.087	15.942	0.9876	0.358
$\Delta a^*$	0-2	-9.9488	38.859	57.176	28.751	0.9832	0.254
	2-4	-9.3831	30.658	41.691	20.623	0.9821	0.259
	4-6	-11.453	37.679	52.825	26.781	0.9686	0.441
	6-8	-16.638	64.404	98.267	50.753	0.9676	0.512
	8-10	-16.098	57.080	86.949	46.426	0.9838	0.347
$\Delta b^*$	0-2	3.0929	12.761	20.194	10.766	0.9461	0.135
	2-4	2.4885	10.248	19.848	12.283	0.8655	0.132
	4-6	2.4054	5.8746	7.9601	4.8993	0.953	0.122
	6-8	3.1118	12.965	23.251	13.151	0.9005	0.121
	8-10	1.9049	6.7371	12.403	7.5797	0.8729	0.129
$\Delta E$	0-2	16.987	47.689	54.331	24.062	0.9867	0.434
	2-4	16.962	57.144	86.876	47.120	0.9882	0.341
	4-6	16.567	47.696	69.492	39.277	0.9807	0.478
	6-8	24.391	78.014	113.06	59.836	0.9835	0.559
	8-10	19.832	49.620	61.434	31.692	0.9899	0.391

In order to obtain data from the images, color calibration was performed for in a single bucket and its value was taken as reference for all other. Also small variation in light distribution was expected during experiments once the imaging box was moved to the next position. Therefore, some variation in the results among various positions could be linked with actual variations in light to that respective position. The average data for color change from all the trays of a bucket would reduce the difference (Amjad and Hensel et al., 2015). Thirdly, the heterogenic nature of the material is also inevitable during the drying process, as biological materials show varying characteristics even with the same operating

conditions due to their heterogenic nature (Nazghelichi et al., 2011).

Curve fitting of empirical data using Sigma-plot 12.3 showed that the polynomial cubic model was best fitted to all studied parameters with higher and lower values of coefficient of determinant ( $R^2$ ) and standard error of estimate (SEE) respectively as shown in Table 1. It can be observed that statistical outputs, i.e. values of standard error of estimate for all the measured ( $\Delta L^*$ ,  $\Delta a^*$  and  $\Delta b^*$ ) and calculated ( $\Delta E$ ) color parameters are following the model fitted data for the respective parameter. 3.3 Color modelling

It was observed from the modelling outputs that first-order model suited to describe  $\Delta L^*$  and  $\Delta b^*$  values with high  $R^2$  while zero order model best to assess the change in  $\Delta a^*$  and total color difference ( $\Delta E$ ). These outputs are strengthened by several studies reporting that the first-order kinetic model was the best for  $L^*$  and  $b^*$  values of double-concentrated tomato paste (Barreiro et al., 1997), kiwi fruits (Muskan, 2001), pineapple (Chutintrasri and Noomhorm, 2007) and peach puree (Avila and Silva, 1999) and zero-order kinetic model was the best for  $a^*$  and total color difference ( $\Delta E$ ) values of kiwi fruits (Muskan, 2001), pineapple (Chutintrasri and Noomhorm, 2007). Figure 8 shows the experimental measured and model predicted values of these color differences by the proposed models, first order model and zero order model.



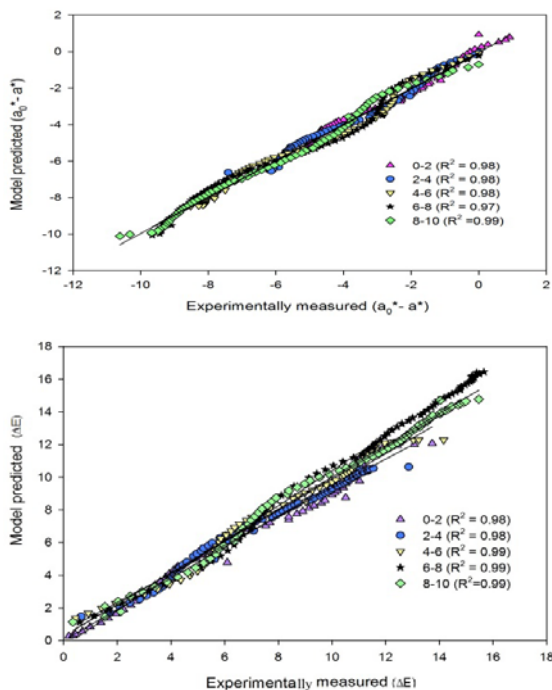


Figure 8 Experimental and model predicted total color difference. First-order kinetic model for  $\Delta L^*$  (A),  $\Delta b^*$  (B) and zero-order kinetic model for  $\Delta a^*$ (C), and  $\Delta E$  (D)

The kinetic constants for all color parameters ( $L^*$ ,  $a^*$ , and  $b^*$ ) using both first and zero kinetic models were almost similar for different positions of the dryer. This shows that change in color parameters was uniform throughout drying compartment due to uniform temperature as the kinetic rate constant mainly affected by drying temperature (Lozano et al., 2000). Using this unit to conduct more experiments under different drying conditions would lead towards accurate optimization of the drying process. Table 2 shows tabulated values of estimated kinetic parameters and statistical results.

**Table 2 Parameters for zero-order and first-order kinetics models for  $L^*$ ,  $a^*$ ,  $b^*$  and total-color difference ( $\Delta E$ )**

Drying Temperature (°C)	Parameters	Sect ion	Zero Order Model			First Order Model			
			* $k_0$ (hr <sup>-1</sup> )	** $C_0$	R <sup>2</sup>	* $k_1$ (1/hr)	** $C_0$	R <sup>2</sup>	
60	$L^*$ (Lightness-darkness)	0-2	-	83.2	0.9	-	83.3	0.9	
			3.538	110	727	0.045	000	752	
		2-4	-	82.2	0.9	-	82.2	0.9	
			2.220	291	659	0.028	512	665	
		4-6	-	84.2	0.9	-	84.3	0.9	
			2.953	960	595	0.036	323	604	
		6-8	-	84.5	0.9	-	84.6	0.9	
			4.419	551	808	0.056	701	908	
		8-10	-	85.4	0.9	-	85.5	0.9	
			3.547	751	808	0.044	536	907	
		$a^*$ (Redness-greenness)	0-2	-	12.9	0.9	-	13.0	0.9
				1.659	230	826	0.111	358	748
			2-4	-	12.9	0.9	-	13.0	0.9
				1.677	780	838	2	802	669

$b^*$ (Yellowness/blueness)	4-6	2.410	86	829	0.176	172	758
	6-8	2.211	910	824	0.170	984	806
	8-10	-	11.2	0.9	-	11.3	0.9
		2.023	850	903	0.158	702	886
	0-2	-	37.4	0.9	-	37.4	0.9
$\Delta E$ (Total color difference)	2-4	0.129	860	317	0.004	812	506
	4-6	-	36.8	0.9	-	36.8	0.9
	6-8	0.125	480	849	0.003	339	961
	8-10	-	35.3	0.7	-	35.3	0.8
		0.149	480	885	0.004	465	897
$\Delta E$ (Total color difference)	0-2	3.438	0.55	0.9	0.58	0.9	
	6	56	820	1.317	80	281	
	2-4	2.637	1.25	0.9	0.55	0.9	
	3	45	781	0.721	37	191	
	4-6	3.790	1.06	0.9	0.48	0.8	
	0	06	834	0.920	64	563	
	6-8	4.813	0.72	0.9	0.59	0.9	
	7	98	907	0.960	01	023	
	8-10	3.931	0.80	0.9	0.44	0.8	
	6	95	923	0.952	51	831	

\* Rate of change in color with Zero and First order models; \*\* Initial value of color variables at time zero

### 3.4 Shrinkage

Figure 9 represents the dimensionless variations of area of the potato slices versus moisture content ratio. It shows a linear relation between the moisture content ratio and the slice area up to  $X/X_0 \geq 0.3$ , due to faster transfer of surface moisture, then the rate of shrinkage became slow due to slow removal of hygroscopic moisture at the last stage of drying process (Mayor and Sereno, 2004).

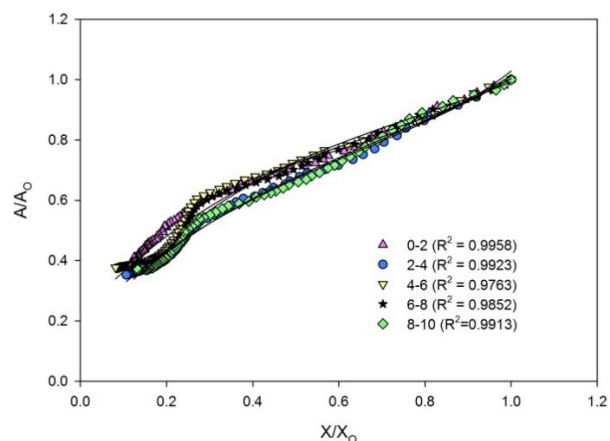


Figure 9 Dimensionless variations of sample area as a function of moisture content ratio

At early stages of drying time, elasticity of cellular potato tissues facilitates higher shrinkage rate in the slices area (Alireza et al., 2009). Although there was a linear

relationship between dimensionless moisture ratio and area ratio, but due to the slight non-linear trend at the end of the drying process, the polynomial cubic model fitted well having higher values of coefficient of determinant ( $R^2$ ).

### 3.5 Data uncertainty

Errors and uncertainties are inevitable during an experiment due to the equipment used, calibration done, observation etc. (Akpınar et al., 2005). An uncertainty analysis was performed for experimentally measured values as well as the model predicted of the color parameters and results are listed in Table 3. The process of error estimation was done using the following equation (Holman, 1994).

$$U = [(x_1)^2 + (x_2)^2 + \dots + (x_n)^2]^{1/2} \quad (4)$$

**Table 3 Uncertainties of the experimental measurements and models predicted color parameters using the movable imaging box**

Experimental measurements					
Parameter	Sections of the drying chamber				
	0-2	2-4	4-6	6-8	8-10
Sample weight (load cell)	±0.451	±0.459	±0.491	±0.440	±0.417
Shrinkage calculation	±1.768	±2.212	±2.088	±1.981	±1.997
Initial color values					
$L_o^*$	±0.264	±0.268	±0.258	±0.263	±0.261
$a_o^*$	±1.088	±1.752	±1.081	±1.214	±1.165
$b_o^*$	±0.604	±0.607	±0.606	±0.615	±0.625
Color values at time interval					
$L^*$	±1.126	±1.100	±1.085	±1.128	±1.091
$a^*$	±1.763	±2.184	±2.537	±2.614	±2.451
$b^*$	±1.357	±1.392	±1.409	±1.430	±1.447
Model predicted					
Initial color values	0-2	2-4	4-6	6-8	8-10
$L_o^*$	±0.120	±0.119	±0.117	±0.117	±0.116
$a_o^*$	±0.445	±0.772	±0.923	±0.967	±0.944
$b_o^*$	±0.266	±0.275	±0.271	±0.279	±0.282
Color values at time interval					
$L^*$	±1.126	±1.101	±1.084	±1.127	±1.091
$a^*$	±1.198	±1.183	±1.938	±1.114	±1.251
$b^*$	±1.242	±1.688	±1.135	±1.726	±1.845

These results show that the imaging system is capable to measure the respective color values, shrinkage and sample weight measurements in acceptable variations which are similar to all the sections of the drying chamber. So shifting of the system did not impart much effect on the measurements. The small variations could be due to the actual variations in the lightness of

respective positions and the heterogeneity of the raw material.

## 4 Conclusion

The digital imaging allows non-invasive measurements and analyses of the food quality parameters that are adequate for food engineering research. A shift able imaging system was developed to investigate the quality changes non-destructively during hot air drying of food material in large convective dryers i.e. batch tray dryer and tunnel dryer. The functionality of this imaging system was assessed by applying it to a diagonal-batch dryer using potato slices (5 mm thick, 60°C drying temperature). Product weight, color and shrinkage measurements were concluded by using the imaging box setup which allowed quantifying representatively and precisely the quality assessment. The quadratic regression model was precisely employed to characterize the relationships of the product color and shrinkage with the moisture ratio ( $X/X_o$ ). This shows that the quality attributes of a product being dried can be measured effectively in real-time by this imaging system. Therefore, under different drying conditions, the detailed understanding of the various changes in product quality would help to optimize the drying process.

The initial results of this system are quite encouraging and can be improved in further study with respect to its flexible application in different food drying processes and spatial light variations when it moves.

## Acknowledgements

The authors would like to express their appreciation to the German Academic Exchange Service (DAAD) and Core Organic Plus Program for financial support in the framework of the SusOrganic-Development of quality standards and optimized processing methods for the organic produce project (Nr: 2814OE006).

## References

Abdullah, M. Z., L. C. Guan, K. C. Lim, and A. A. Karim. 2004. The applications of computer vision systems and

- tomographic radar imaging for assessing physical properties of food. *Journal of Food Engineering*, 61(1): 125–135.
- Akpinar, E. K., A. Midilli, and Y. Bicer. 2005. Energy and exergy of potato drying process via cyclone type dryer. *Energy Conversion and Management*, 46(15-16): 2530-2552.
- Alireza, Y., L. Acefeh, and M. Reza. 2009. New method for determination of potato slice shrinkage during drying. *Computer and Electronics in Agriculture*, 65(2): 268-274.
- Amjad, W., A. Munir, A. Esper, and O. Hensel. 2015. Spatial homogeneity of drying in a batch type food dryer with diagonal air flow design. *Journal of Food Engineering*, 144(jan): 148-155.
- Amjad, W., O. Hensel, and A. Munir. 2015. Batch drying of potato slices: kinetic changes of colour and shrinkage in response of uniformly distributed drying temperature. *CIGR Journal*, 17(3): 296-308.
- Avila, I. M., L. B., and C. L. M. Silva. 1999. Modelling kinetics of thermal degradation of colour of peach puree. *Journal of Food Engineering*, 39(2): 161-166.
- Barreiro, J. A., M. Milano, and J. A. Sandoval. 1997. Kinetics of color change of double concentrated tomato paste during thermal treatment. *Journal of Food Engineering*, 33(3): 359-371.
- Chen, X. D., and A. S. Mujumdar. 2008. *Drying Technologies in Food Processing*. Oxford, UK: Blackwell Publishing.
- Chua, K. J., M. N. A. Hawlader, S. K. Chou, and J. C. Ho. 2002. On the study of time-varying temperature drying—effect on drying kinetics and product quality. *Drying Technology*, 20(8): 1559–1577.
- Chutintrasri, B., and A. Noomhorm. 2007. Colour degradation kinetics of pineapple puree during thermal processing. *LWT - Food Science and Technology*, 40(2): 300-306.
- Contreras, C., M. E. Martin-Esparza, A. Chiralt, and N. Martinez-Navarrete. 2008. Influence of microwave application on convective drying: effects on drying kinetics and optical and mechanical properties of apple and strawberry. *Journal of Food Engineering*, 88(1): 55–64.
- Diamante, L., M. Durand, G. Savage, and L. Vanhanen. 2010. Effect of temperature on the drying characteristics, colour and ascorbic acid content of green and gold kiwifruits. *International Food Research Journal*, 17(2): 441-451.
- Elamin, O. M. A. 2014. Effect of drying temperature on some quality attributes of mango slices. *International Journal of Innovation and Scientific Research*, 4(2): 91-99.
- El-Masry, G., S. Cubero, E. Moltó, and J. Blasco. 2012. In-line sorting of irregular potatoes by using automated computer-based machine vision system. *Journal of Food Engineering*, 112(1-2): 60–68.
- Farias, A. M., and C. Ratti. 2008. Dehydration of foods. In *Advances in Food Dehydration*, ed. C. Ratti, 1–36. Boca Raton: CRC Press.
- Fernandez, L., C. Castellero, and J. M. Aguilera. 2005. An application of image analysis to dehydration of apple discs. *Journal of Food Engineering*, 67(1/2): 185–193.
- Finlayson, D. G., M. M. Darrodi, and M. Mackiewicz. 2015a. The alternating least squares technique for nonuniform intensity color correction. *Color Research and Application*, 40(3): 232–242.
- Finlayson, G., M. Mackiewicz, and A. Hurlbert. 2015b. colour correction using root-polynomial regression. *IEEE Transactions on Image Processing*, 24(5): 1460-1470.
- Groß, F., R. Benning, U. Bindrich, K. Franke, V. Heinz, and A. Delgado. 2011. Optical online measurement technique used for process control of the drying step during pasta production. *Procedia Food Science*, 1(1): 1301-1308.
- Hassankhani, R., and H. Navid. 2012. Potato sorting based on size and color in machine vision system. *Journal of Agricultural Science*, 5(4): 235-244.
- Hatamipour, M. S., H. H. Kazemi, A. Nooralivand, and A. Nozarpoor. 2007. Drying characteristics of six varieties of sweet potatoes in different dryers. *Food and Bioprocess Processing*, 85 (C3): 171–177.
- Holman, J. P. 1994. *Experimental Methods for Engineers*. 6th ed. Singapore: McGraw-Hill.
- Jayas, D. S., J. Paliwal, and N. S. Visen. 2000. Multi-layer neural networks for image analysis of agricultural product. *Journal of Agricultural Engineering Research*, 72(2): 119–128.
- Khraisheh, M. A. M., T. J. R. Cooper, and T. R. A. Magee. 1997. Shrinkage characteristics of potatoes dehydrated under combined microwave and convective air conditions. *Drying Technology*, 15(3/4): 1003–1022.
- Krokida, M. K., E. Tsami, and Z. B. Maroulis. 1998. Kinetics of colour changes during drying of some fruits and vegetables. *Drying Technology*, 16(3–5): 667–685.
- Leon, K., M. Domingo, F. I. Pedresch, and J. Leon. 2006. Color measurement in L\*a\*b\* units from RGB digital images. *Food Research International*, 39(10): 1084-1091.
- Lozano, J. E., C. Anon, and G. V. Barbosa-Canovas. 2000. *Trends in Food Engineering*. USA: Technomic Publisher.
- Mahendran, R., G. C. Jayashree, and K. Alagusundaram. 2012. Application of computer vision technique on sorting and grading of fruits and vegetables. *Journal of Food Processing and Technology*, S1: 1-8.
- Martynenko, A. 2006. Computer vision system for control of drying process. *Drying Technology*, 24(7): 879–888.
- Mayor, L., and A. M. Sereno. 2004. Modeling shrinkage during convective drying of food materials: a review. *Journal of Food Engineering*, 61(3): 373-386.
- Mclaughlin, C. P., and T. R. A. Magee. 1998. The effect of shrinkage during drying of potato spheres and the effect of drying temperature on vitamin C retention. *Food and Bioprocess Processing*, 1998, 76(3):138-142.

- Mendiola, R. C., H. S. Hernandez, J. C. Perez, L. A. Beltran, A. J. Aparicio, P. Fito, and G. F. Lopez. 2007. Non-isotropic shrinkage and interfaces during convective drying of potato slabs within the frame of the systematic approach to food engineering systems (SAFES) methodology. *Journal of Food Engineering*, 83(2): 285-292.
- Mujumdar, A. S. 2000. *Drying Technology in Agricultural and Food Science*. Plymouth, UK: Science Publishers Inc.
- Mujumdar, A. S., and C. L. Law. 2009. Drying technology: trends and applications in postharvest processing. *Food and Bioprocess Technology*, 3(6): 843e852.
- Mulet, A., J. Garcia-Reverter, J. Bon, and A. Berna. 2000. Effect of shape on potato and cauliflower shrinkage during drying. *Drying Technology*, 18(6): 1201-1219.
- Muskan, M. 2001. Kinetics of colour change of kiwifruits during hot air and microwave drying. *Journal of Food Engineering*, 48(2): 169-175.
- Narendra, V. J., and K. S. Hareesh. 2010. Prospects of computer vision automated grading and sorting systems in agricultural and food products for quality evaluation. *International Journal of Computer Applications*, 1(4): 1-12.
- Nazghelichi, T., M. Aghbashlo, M. H. Kianmehr, and M. Omid. 2011. Prediction of energy and exergy of carrot cubes in a fluidized bed dryer by artificial neural networks. *Drying Technology*, 29(3): 295-307.
- Nunez, V. A. M., B. Sturm, and W. Hofacker. 2016. Simulation of the convective drying process with automatic control of surface temperature. *Journal of Food Engineering*, 170:16-23
- Orikasa, T., L. Wu, T. Shiina, and A. Tagawa. 2008. Drying characteristics of kiwifruit during hot air drying. *Journal of Food Engineering*, 85(2): 303-308.
- Pathare, P. B., U. L. Opara, and A. J. Al-Said. 2012. Colour measurement and analysis in fresh and processed foods: A review. *Food Bioprocess Technology*, 6(1): 36-60.
- Pedreschi, F., J. Leo'n, D. Mery, and P. Moyano. 2006. Development of a computer vision system to measure the colour of potato chips. *Food Research International*, 39(10): 1092-1098.
- Pedreschi, F., J. Leo'n, D. Mery, P. Moyano, R. Pedreschi, K. Kaack, and K. Granby. 2007. Colour development and acrylamide content of pre-dried potato chips. *Journal of Food Engineering*, 79(3): 786-793.
- Ramos, I. N., C. L. M. Silva, A. M. Sereno, and B. J. M. Aguilera. 2004. Quantification of microstructural changes during first stage air drying of grape tissue. *Journal of Food Engineering*, 62(2): 159-164.
- Sahin, S., and S. G. Sumnu. 2006. *Physical Properties of Foods, Food Science Text Series*. New York: Springer Science Business Media, LLC.
- Segnini, S., P. Dejmek, and R. O'ste. 1999. A low cost video technique for colour measurement of potato chips. *Lebensmittel-Wissenschaft und-Technologie*, 32(4): 216-222.
- Shekofteh, M., F. E. Cherati, S. Kamyab, and Y. Hosseinpor. 2012. Study of shrinkage of potato sheets during drying in thin-layer dryer. *Research Journal of Applied Sciences, Engineering and Technology*, 4(16): 2677-2681.
- Sturm, B. 2010. Influence of process control on drying kinetics and product attributes of sensitive biological products. *Forschungsbericht Agrartechnik*, 491(1): (1-197).
- Sturm, B., N. V. Anna-Maria, and W. C. Hofacker. 2014. Influence of process control strategies on drying kinetics, colour and shrinkage of air dried apples. *Applied Thermal Engineering*, 62(2): 455-460.
- Sturm, B., W. Hofacker, and O. Hensel. 2012. Optimizing the drying parameters for hot air dried apples. *Drying Technology*, 30(14): b570-1582.
- Wang, N., and J. G. Brennan. 1995. Changes in structure, density and porosity of potato during dehydration. *Journal of Food Engineering*, 24(1): 61-76.
- Yam, K. L., and S. E. Papadakis. 2004. A simple digital imaging method for measuring and analyzing color of food surfaces. *Journal of Food Engineering*, 61(1): 137-142.